

# A Futuristic Approach to Synaptic Fusion of Inn and CNN Architectures for Tissue Classification

K.Chandrasekhar, P.Vijaya Kumari, C.Prabhavathi, D.Raghunath Kumar Babu, S.Ghouhar Taj

Assistant Professor(Adhoc)CSE Department,JNTUACEP,chandra507shiva@gmail.com

Assistant Professor(Adhoc)CSE Department,JNTUACEP, vijaya.jntuacep@gmail.com

Assistant Professor(Adhoc)CSE Department,JNTUACEP, [prabhavathi1231@gmail.com](mailto:prabhavathi1231@gmail.com)

Assistant Professor(Adhoc)CSE Department,JNTUACEP, [raghunath.d29@gmail.com](mailto:raghunath.d29@gmail.com)

Assistant Professor(Adhoc)CSE Department,JNTUACEP,sgtaj786@gmail.com

**Abstract**— Radiology refers to a branch of medical specialization that focuses on image processing for diagnostics. It has seen immense advances in predictive methodologies in the past few decades, with its predictive capacities being mostly accounted for by machine learning and deep learning approaches. However, classical machine learning has shown comparatively poor performance with regard to non-linear, irrelevant, and highly correlated features in data, and has also shown high reliance on proper presentation of data. This paper aims to improve that notion and aid radiological diagnostics using advanced deep learning and image processing techniques, which will eventually result in improved diagnostic accuracy and productivity of radiologists. This experiment efficiently fuses hybrid neural networks by using CNN (Convolutional Neural Network Architecture) and INN (Involutorial neural networks) architectures, which was then compared with other pre-trained models, trained and tested on multiple color models such as RGB (Red, Green, Blue), HSV (Hue, Saturation, Value), and YCbCr (Luminance, Chrominance), to get optimal efficiency. Our proposed Convolutional Neural Network architectures, which include two fused hybrid models of INN and CNN, when trained with carefully handcrafted features, outperform other pre-trained models in terms of micro accuracy.

**Keywords**— *Tissue Classification, INN, CNN, Fusion Networks, Deep learning.*

## I. INTRODUCTION

The cell is the most primitive form of life, capable of asexual reproduction, and numerous functionalities including regulation, maintenance, and regeneration. There is a spectacular chemical processing unit inside the area that the membrane defines as its bounds [1]. Highly developed multicellular animals and plants have specialized tissues that can plan and control an organism's response to its environment. In multicellular bodies, cells create a variety of tissues. Living beings have four different types of tissues: connective tissue, epithelial tissue, muscle tissue, and nerve tissue. Organ development in the body involves a variety of tissue types [2].

Tissue engineering is the procedure by which mixing of scaffolds, cells and physiologically active chemicals, is done, together. Damaged tissues can be repaired, improved and regenerated by assembly of useful constructions. Regenerative medicine involves self-healing studies, and

tissue engineering in its comprehension. Tissue engineering and regenerative medicine are now mainly used in an exchangeable manner, as the profession seeks to focus on cures instead of treatments for complex, often chronic, diseases. Hence, improving classification of cells and tissues can further aid the field of tissue engineering and regenerative medicine [3].

The domains of radiology, and medical imaging has seen tremendous advances in perspective of image processing and digital imaging. Digital radiology is used to diagnose pathological diseases and abnormalities by scanning images. Computational pathology is also a technique used frequently, to aid pathologists in this task, and can be used further to detect cancer, characterize neo vascularization, detect and classify micro lesions, and much more [4]. In this study, multiple state-of-the-art models have been trained on the ADP dataset, with and without using various color models such as RGB, HSV etc. As in most cases, CNN alone can turn out to be the best solution, hence multiple CNN pre-trained and tested architectures like vgg16 [5], mobilenet2 [6], inceptionresnet3 [7], 2 have been used in this study. Two more custom CNN models which were designed to fit this particular dataset in some cases perform better than the state-of-the-art pre-trained models mentioned above in terms of accuracy.

This paper has been sectioned into six components. The first section being the introduction section and the second being the literature review section with a report on related works. The third section provides details of the dataset used, the fourth section briefs the technologies used in the paper and the fifth section details the experiment procedure and analysis derived from it. The sixth section is the acknowledgement section, followed by the reference section which contains a list of the referred works.

## II. LITERATURE REVIEW

The field of healthcare has seen immense involvement and development of machine learning in integration to itself, in the past years. Particularly, in fields of cancerous tissue and tumor tissue [8] classifications, deep learning models have been used and implemented extensively. In 2020, L. Saba et al. proposed a computer aided model which used optimal transfer learning approaches, namely MobileNet and Visual Geometric Group-19 (VGG-19) to detect tissues causing Wilson's disease [9]. In 2021, again, L. Saba et al. developed

four machine learning, one deep learning and one transfer learning architectures to characterize tissues. The mean accuracies for DL, TL, and ML over the mean of the three data sets using K10 (9:1 training to testing) were 93.55%, 94.55%, and 89%, respectively [10]. Marta Sbalgiara et al. implemented a risk-assessment scheme using a NTRK inhibition [11]. An automated process for classification of histological slides of both brain and breast tissues, utilizing Google Inception V3 Convolutional Neural Network (CNN), was proposed by Justin Ker et al. The team reported a successful automated classification technique for brain histology specimens into low grade glioma (LGG), or high grade glioma (HGG). Their F1 score reported an improvement from 0.57 to 0.913 [12]. Juan S. Lara et al. explored an automated fusion approach (multi-modal) for classification and retrieval of prostate histopathology images /WSIs. The approach exploited a weakly supervised machine learning model which combined a bag-of-features representation, deep learning, and kernel methods. It performed excellently with an accuracy of 77.01%, thus increasing the baseline performance in WSI cancer detection by 4.74% [13]. In 2019, Quoc Dang Vu et al. proposed two machine learning algorithms, one designed for segmentation of nuclei and the other one for classification of whole slide tissue images. The segmentation technique explored a multiscale deep residual aggregation network, and classification algorithm first implemented a patch level classification technique, followed by implementation of a Random Forest Classifier to improve accuracy. The segmentation and classification algorithms achieved accuracy scores of 78% and 81% respectively [14]. More recently, in 2022, Shan Lin et al. proposed a novel, comprehensive surgical perception framework, Semantic Super, which combined semantic and geometric information to aid data association, 3D reconstruction and endoscopic scene tracking. The proposed framework was demonstrated on challenging endoscopic data with deforming tissue, highlighting its advantages [15]. In even more recent light, N. Dasari et al. developed a multi-scale CNN for early detection of Interstitial Lung disease tissues. The model's inputs were enhanced using Gabor filter, which aided its outstanding performance with an accuracy of 99.67% [16].

Xuan Liu et al. devised a technique for automated skin tissue classification, based on optical coherence tomography (OCT). The team implemented a deep CNN with U-Net architecture for skin segmentation, utilizing the U-Net as a feature extractor in the processor. They also used SVM for detecting abnormalities in the data [17]. An end-to-end framework using deep learning techniques was proposed by H.G. Nyugen et al. in 2020. The proposed model was trained to classify TMA spots into three categories: normal, epithelium and tumor tissue types. The model was an integration of two effective deep learning architectures, CNN and capsule Network [18].

Deep learning methodologies, particularly CNN and various CNN based architectures, including transfer learning have been explored extensively in terms of tissue classification. The results vary according to the architecture used, and quite a few number of proposed techniques include segmentation and classification both, under a single experiment of tissue classification.

### III. DATASET

This component is divided further into two sections, A and B, Dataset details and Dataset preprocessing respectively.

#### A. Dataset Details

From a sample match of 500 glass slides, each measuring 1" X 3", a total of 100 were carefully selected. The selected slides were then scrutinised under equipment with a 20x objective lens and 0.75 numerical aperture, and they were further chosen based on the slides' few focus variations, the stains' wider range of colour variations, the origin organs, and the diagnoses (disease / non-disease) they contained.

Following a scan of those 100 chosen slides, each slide was transformed into particular randomised subgroups of non-background patches with a diameter of 1088 by 1088 pixels, containing an overlap with 32 pixels. In all, 17,668 patches were accumulated. Background patches, which had greater than 97.5% of pixels, and intensities greater than 85%, in all three RGB channels, were exempted. Patches with obvious focus issues or non-tissue items, that lacked any distinguishable tissue were also removed. Each glass slide yielded an average of 177 patches (from 12 to 280).

To achieve uniform labelling, the following labelling standards were used:

- When the possibility of tissue being present anywhere in the patch, in any possible quantity, is high, non-cellular labels, or labels with singular format, are assigned;
- Cellular labels, i.e., labels with names in plural format, (e.g. "Erythrocytes") were assigned to those patches, which had cells determined to be present anywhere in it, in quantities of 5 or more. The labels were assigned at highest specificity possible;
- Each pixel, while only correspondent to one particular morphological type, can correspond to another cell functionality
- Labels were allotted at most primitive levels.
- Patches with no distinguishable tissue structures were excluded from the database.

Three levels of tissue type classification are included in the collection. The top levels have their types assigned as "Glandular" and "Transport Vessel" tissues, as well as seven morphological tissue types (a superset of five fundamental types in, and four fundamental kinds in). Each top-level tissue type in the taxonomy is further broken down into more precise sub-types, each of which either correlates to or does not correspond to a visibly distinguishable tissue type. "Undifferentiated" child node tissues were connected with the parent tissues nodes in situations where a more particular child node type could not be found, but we did not consider such nodes to be part of that level (due to its insufficient specificity).

#### B. Dataset Preprocessing

A total of 17,668 patches were collected and analyzed. The first level consists of 9 classes: Skeletal (S), Epithelial (E), Connective Proper (C), Blood (H), Adipose (A), Muscular (M), Nervous (N), Glandular (G). Because of the multi-labelled nature of the dataset, one patch has the possibility of belonging

tooneor more classesand labels.Thisissuecanbe resolved withthehelpofclassweightedclassification,whichwasfirst proposed by the Ziyu Xu et al. [19]

These datasets have a disproportionately high concentrationofonetypeofdatacomparedtoanother.When dealingwithsuchunbalanceddatasets,weightedclassification is frequently utilized. It is simple to obtain a high accuracy with such datasetsbymisclassifying points from the smaller class.Itisnotaverygoodconcepttomisclassifymembersof thesmallerclassinorderto"sacrifice"theminfavourofthose in the larger class. Utilizinga weighted classification cost to change the learned classifier's behavior, such that it gives moreweighttopointsintheminorityclassandlessweightto points inthe majorityclass, isone technique used to address thisproblem.Itisusualpracticetogiveweights,suchthatthey areinverselyproportionatetothenumberofmembersofeach class in order to achieve this result. Concisely, first observe that $P=|+1|+1$ ,ifwedenote $+1$ and $1$ indexsetsforthe points inclasses $+1$ and $1$ , respectively.These class-wise weights can thenbesettobeinverselyproportionaltothenumberofpoints in each class by indicating  $+1$  and  $1$  as the weights for each memberofclasses $+1$ and $1$ , respectively.Theassignmentof weights in classes is done as shown in eq. 1, and 2.

$$\beta+1 = \frac{1}{|\alpha+1|} \tag{1}$$

$$\beta-1 = \frac{1}{|\alpha-1|} \tag{2}$$

TABLE I. SIZES OF TRAINING, TESTING AND VALIDATION DATA

General Information	
Trainingsamples	14134
Validationsamples	1767
Testsamples	1767
Originaldimension	1080x1080
Level1classes	9

TABLE II. WEIGHTS GIVEN TO EVERY CLASS

Label	Weight
Epithelial	1.64597648
ConnectiveProper	1.35538934
Blood	1.79867651
Skeletal	32.71759259
Adipose	26.46816479
Muscular	3.5718979
Nervous	7.59484148
Glandular	2.25243028

Table I contains information about the data-set sample size includingtrainingset,validationsetandtestingsetandtable II contains information about the weight of classes . Three distinctcolourconfigurationsknownas'colourspace',have beenusedontheinputforbetterprocessing,namelyYCbCr, RGB and HSV.

IV. TECHNOLOGIES/SOFTWARE

Sincedeeplearning(DL)isarelativelynewfieldofstudy, it isimpossibleto provideacomprehensivereviewof all the publishedresearchonhistopic.Therefore,wehavefocused on the most important and related works.

A. Convolutional Neural Networks (CNN)

CNN or Convolution neural networks are a collection of deep learning networks that are primarily used for detection and classification of images. It also aids dimensionality reduction and its layers work on principles of feature extraction, which eliminates the need for implementing manual feature extraction further into the process. The input usuallyconsistsofimageswhichhaseither3channels(RGB) or1channel(GreyScale),andtheseimagesarerepresentedin matrixformswithashapeconsistingofitschannelsizeasthe last parameter. The network uses a mathematical operation, convolution,whichmultiplieseachcorrespondingelementin thematrix,toanelementinthekernel,andsumseachproduct to give the convoluted output, which is kept in a dimension-reducedmatrix.Theirapplicationsexendtohealthcare[20], agriculture[21],security[22],andmanymoreusecases.Their basic architecture is given below in fig 1.

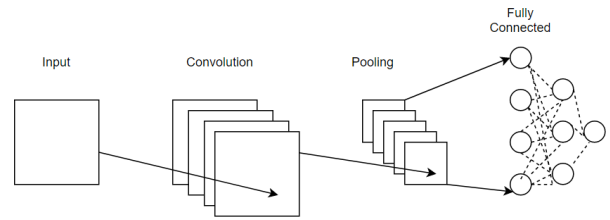


Fig.1. Typical CNN Architecture

A typical CNN consists of 4 main types of layers – Convolution, Pooling, Flattening, and Fully-Connected. Each of these layers serves to extract features, reduce spatial dimensions, convert 2d matrix to linear vectors, and to find probability of the image belonging to a particular class, respectively.Mathematically,convolutionholdstheproperty of translation equivalence, as depicted in eq 3. This implies thatcharacteristicsoftheoriginalfunctioncanbeconfigured intoanewfunction.Convolutionoperationonimage matrices can be depicted mathematically via eq 4.

$$a(b(n))=b(a(n)) \tag{3}$$

$$f * g[m] = \sum f[m-i]g[i] \tag{4}$$

Activation functions like Tanh and ReLU are used in the Fully-Connected layer, which is made using ANN(Artificial NeuralNetworks),todetermine the probabilityoftheoutput classification

B. Involutional Neural Networks (INN)

Involutioniscapableofusingself-attentiontoincorporate spatial model and enhance image classification.It takes advantage of nonlinear transformations in the spatial and channel domain with inverse properties G, and is uniquely designedforthe pixel $X_{i,j,R,C}$ .Thismechanismisutilized to manage and maintain the groups of images where each groupusesaninvolutionkernel.Thefeaturemapoutputtedby theusageofsuchinvolutionkernelisobtainedbyperforming Multiply – Add operations, which are specified as shown in eq 5.

$$Y = \sum_{(u,v) \in \Delta(k)} H \sum_{i,j,u+l_2,v+l_2} \frac{K \times K}{|C|} X_{i+u,v+k} \tag{5}$$



The input feature map, suppose  $X$ , determines the form of the convolution kernels  $H$ , which are then trained on the original input tensors to ensure that the output kernels are comfortably aligned with the input. The functional mapping at each point  $(i, j)$  is abstracted, while the kernel-generating function is represented by the symbol  $H_{i,j}$ , which is formulated as shown in eq 6.

$$H_{i,j} = \phi(\Psi_{i,j}) \tag{6}$$

where  $\Psi_{i,j}$  stores indices of the set of pixels,  $H_{i,j}$  is conditioned on. The kernel generation function, as displayed in eq. 7.

$$\phi: \mathbb{R}^C \rightarrow \mathbb{R}^{K \times K \times G} \tag{7}$$

with,  $\Psi_{i,j} = \{(i,j)\}$  taking the form shown in eq 8.

$$H_{i,j} = \phi(x_{i,j}) = w_1 \sigma(w_0 x_{i,j}) \tag{8}$$

This particular formula assumes the implementation of Batch normalization, as well as non-linear activation functions.  $W_0, R, C_r, C$ , and  $W_1, R, (K \times K \times G) C_r$  depict two linear transformations as shown in equations 9 and 10, that constitute a bottleneck architecture, where the intermediate channel dimension is affected by reduction ratio  $r$ , for convenient processing.

$$W_0 \in \mathbb{R}^{r \times C} \tag{9}$$

$$W_1 \in \mathbb{R}^{(K \times K \times G) * \left(\frac{C}{r}\right)} \tag{10}$$

The network replicates ResNet's [23] design across the full network with convolution by stacking blocks which are residual, on top of each other, since ResNet's architecture makes it suitable for testing out new concepts and comparing results. The neural network often experiences significant redundancy once spatial and channel information interact. During the kernel generation step, information stored in the dimensions of the kernel is scattered into its spatial neighborhood. Subsequently, the information in an enriched receptive field is gathered with the help of the enormous and dynamic convolution kernels. The addition of the attention mechanism improved the performance of the encoder-decoder paradigm for machine translation.

### V. RESULTS AND ANALYSIS

This section provides the testing and findings from the dataset using multiple designs with various parameter combinations.

The best design for categorization with the lowest computing cost was selected. The experiments and findings are covered in Section A, and the assessment of the chosen architecture is covered in Section B.

#### A. Experimental Proceedings

In this study, we have experimented with various combined architectures, fusing both CNN and INN. After intense explorations of the hyperparameters, the model was trained and tested on large data to obtain the optimal architecture. In CNN, inputs are passed on basis of the shape of the features passed, and feature extraction is applied

accordingly. Two variations of the experiment were carried out. In CNN, the kernel extracts the significant features by comparing and detecting rough patches in the image, with the help of a filter / kernel. These features are represented as a matrix which is then passed to the fully connected layer for further processing and classification. In INN, feature extraction is performed by instantiating the kernel / filter at every pixel, hence taking the pixel's parameters and conditions into account.

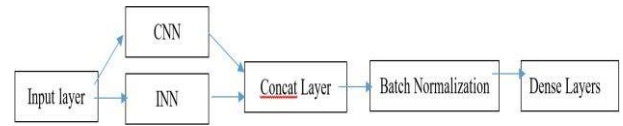


Fig.2. Variation 1, Input is passed parallelly to INN and CNN



Fig.3. Variation 2, Input is passed to CNN layer, then to the INN layer

Figures 2 and 3 depict the two variations of the architecture devised for this experiment. In figure 3, the first variation, the input matrix/ image is passed to the CNN and INN layers simultaneously. The features extracted from both networks are then combined into a new matrix and provided as input to the Concatenation layer for further processing. In figure 4, the second variation, the input matrix is first passed to the CNN layer, which outputs a feature probability matrix. This matrix is then provided as input to the INN layers, and the output derived from this processing, is sent into the Dense layers of the fully connected layer for classification. For this experiment, we determined the first architecture, shown in fig 2, to work better than the second. Hence, all recorded results are for optimized versions of the first architecture. After finalizing the architecture, we conducted further experiments by tweaking other parameters such as variation in number of layers present in the CNN, ANN and INN, alongside regularization levels including L1 regularization and L2 regularization, image input sizes (IS), batch norm (BN), dropout layers (DO), kernel sizes (KS), and pooling matrix sizes (PS) which later on judged on the criteria such as Binary accuracy (BA), Binary cross-entropy loss (BCEL), and time taken (TT) for training. The standard loss function used in classification is cross entropy loss, which was incorporated into the CNN in accordance to eq. 11.

$$Loss = \frac{1}{n} * \sum(w_j * y_j * \log(y_{pred_j})) \tag{11}$$

In the above equation,  $w_j$  refers to the weight of the  $j^{th}$  observation,  $n$  addresses the number of samples, and  $y_j$  refers to the actual value of the  $j^{th}$  observation. We downstream trained these two architectures with 5 different configurations by tweaking the above hyperparameters, for 40 epochs each, and obtained optimal results with ICNN-4, which provided the highest BA and lowest BCEL. Table 3 shown below, contains the results of all the configured architectures.

TABLE III. RESULTS RECORDED FROM CNN, INN ARCHITECTURES

S.I	CL	AL	INN	IS	Regularization		INN configuration					CNN configuration			BCEL	VBA	
					L1	L2	DO	C	KS	S	RR	GN	KS	PS			S
1	2	2	2	(128x128)	no	no	no	3	3	1	2	1	(3,3)	(2,2)	2	0.14348	87.3454
2	3	3	3	(128x128)	yes	no	yes	3	3	1	2	2	(9,3)	(4,2)	1	0.23849	83.2399
3	5	3	4	(256x256)	yes	no	no	3	3	1	2	1	(9,3)	(2,2)	1	0.31926	78.4389
4	4	3	3	(128x128)	no	yes	yes	3	3	1	2	1	(3,3)	(2,2)	2	0.1293	90.3264
5	6	4	5	(128x128)	yes	no	no	3	3	1	2	1	(9,3)	(4,2)	1	0.25349	86.4389

B. Results and Analysis:

From the observations recorded above in table III, ICNN-4 gives optimal results as compared to the other models. It acquired a Binary Accuracy of 90.3264, and a Binary Cross Entropy Loss of 0.1293. The formulae used for calculating their precision score, recall score and F1 score have been depicted in equations 12, 13, and 14 respectively [24]. These formulae have been used to calculate the metrics obtained in table V, from corresponding confusion matrices.

$$Precision = \frac{TP}{TP + FP} \tag{12}$$

$$F1\ score = \frac{2 * Precision * Recall}{Precision + Recall} \tag{14}$$

$$Recall = \frac{TP}{TP + FN} \tag{13}$$

Table IV, contains the metrics obtained for all the 9 classes given by our optimal architecture, where 330 non-augmented images were considered for metric evaluation. As data augmentation was used to change the color model of the images and also to resize the image to a certain size, we cannot use enlarged images for evaluation. Therefore we only considered 330 out of 17000 images for better evaluation of our optimal architecture. We also tested the same model on augmented images, but for correct and fair evaluation of the model, only the non-augmented images were considered.

TABLE IV. METRICS FOR ALL 9 METRICS OBTAINED FROM MODEL PERFORMANCE ON THE DATASET

HTT	TPR	FPR	TNR	FNR	ACC	F1	AUC
E	0.8357664234	0.1639344262	0.8360655738	0.1642335766	0.8358800226	0.863336475	0.9158449095
C	0.8408748115	0.1587301587	0.8412698413	0.1591251885	0.8409734012	0.8880923935	0.9165187442
H	0.7830474268	0.2190721649	0.7809278351	0.2169525732	0.7821165818	0.8012390294	0.8622330355
S	0.9818181818	0.001168224299	0.9988317757	0.01818181818	0.9983022071	0.972972973	0.9997557349
A	0.5277777778	0.01002949853	0.9899705015	0.4722222222	0.9711375212	0.5984251969	0.9360373648
M	0.730125523	0.08688906129	0.9131109387	0.269874477	0.8636106395	0.743343983	0.9209792548
N	0.962962963	0.007736943907	0.9922630561	0.03703703704	0.9886813809	0.9541284404	0.9969016405
G	0.897094431	0.09776833156	0.9022316684	0.102905569	0.8998302207	0.8933092224	0.9561887436
T	0.5375816993	0.2225108225	0.7774891775	0.4624183007	0.6943972835	0.5492487479	0.7275358628
Average	0.797954866	0.08229889551	0.9177011045	0.202045134	0.8749921398	0.8199275362	0.8967818685

From the above results, and the ROC curve shown below in figure 4, it is clear that our architecture showed excellent results.

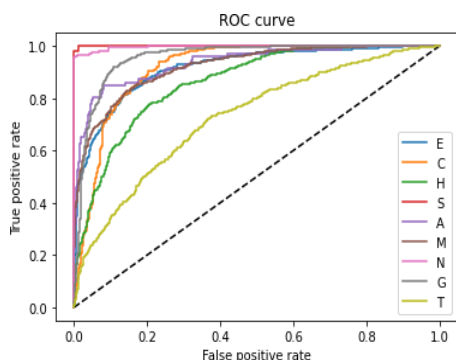


Fig.4. ROC Curve of ICNN-4

VI. CONCLUSION

This paper aimed to combine two highly efficient image classification networks, and fuse them to create a model which provides optimal combinations of losses, precision, recall and F1-score. Out of the 5 different versions of the fusion architecture, which were tested, we configured changes in the number of layers, regularization, input shapes etc. We determined ICNN-4 to be the optimal architecture, based on its simplicity, low computational cost and specifications as stated below in table V. The boundaries and design of the chosen model were easier to configure and provided results which were superior to the other models used for comparison. Overall, hybrid architectures provide more stable, and more efficient performances, as compared to traditional architectures. There is still, however, room for enhancement. Further evolution of AI is guaranteed to show better results.

TABLE V. SPECIFICATIONS OF THE SELECTED ARCHITECTURE

CL	AL	INN	IS	Regularization		INN configuration						CNN configuration			BCEL	VBA	Epoch
				L1	L2	DO	C	KS	S	RR	GN	KS	PS	S			
4	3	3	(128x128)	no	yes	yes	3	3	1	2	1	(3,3)	(2,2)	2	0.1293	90.3264	40

## ACKNOWLEDGMENT

The first author would like to extend their sincere gratitude to all co-authors, especially Prof. M. K. Gourisaria for his guidance and co-operation.

## REFERENCES

- [1] M. Cuffe, John A. Cooper, C. Chow, B. M. Alberts, J. M. W. Slack, W. D. Stein, L. A. Staehelin, M. R. Bernfield, H. F. Lodish and R. A. Laskey, "cell". Encyclopedia Britannica, 18 Oct. 2022.
- [2] Britannica, The Editors of Encyclopaedia. "tissue". Encyclopedia Britannica, 23 Aug. 2022, <https://www.britannica.com/science/tissue>. Accessed 21 November 2022.
- [3] K. Rogers. "tissue engineering". Encyclopedia Britannica, 10 Dec. 2018, <https://www.britannica.com/science/tissue-engineering>. Accessed 22 November 2022.
- [4] A. Abraham, 2005. "Artificial neural networks." *Handbook of measuring system design*.
- [5] P. A. Bautista, N. Hashimoto, and Y. Yagi. "Color standardization in whole slide imaging using a color calibration slide." *Journal of pathology informatics*, 5, 2014. 4323
- [6] A. H. Beck, A. R. Sangoi, S. Leung, R. J. Marinelli, T. O. Nielsen, M. J. V. D. Vijver, R. B. West, M. D. V. D. Rijn, and D. Koller. "Systematic analysis of breast cancer morphology uncovers stromal features associated with survival." *Science translational medicine*, 3(108):108ra113–108ra113, 2011. 4322
- [7] M. Brown, P. Browning, M. W. Wahi-Anwar, M. Murphy, J. Delgado, H. Greenspan, F. Abtin, S. Ghahremani, N. Yaghmai, I. da Costa, et al. "Integration of chest CT into the clinical workflow and impact on radiologist efficiency." *Academic radiology*, 2018. 4321
- [8] V. Singh, M. K. Gourisaria, H. GM, S. S. Rautaray, M. Pandey, M. Sahni, E. Leon-Castro and E. F. Espinoza-Audelo, 2022. "Diagnosis of intracranial tumors via the selective CNN data modeling technique." *Applied Sciences*, 12(6), p.2900.
- [9] L. Saba, M. Agarwal, S. S. Sanagal, S. K. Gupta, G. R. Sinha, A. M. Johri, ... & J. S. Suri (2020). "Brain MRI-based Wilson disease tissue classification: An optimized deep transfer learning approach", *Electronics Letters*, 56(25), 1395-1398.
- [10] L. Saba et al., "A Multicenter Study on Carotid Ultrasound Plaque Tissue Characterization and Classification Using Six Deep Artificial Intelligence Models: A Stroke Application," in *IEEE Transactions on Instrumentation and Measurement*, vol. 70, pp. 1-12, 2021, Art no. 2505312, doi: 10.1109/TIM.2021.3052577.
- [11] M. Sbaraglia, E. Bellan, and A. P. D. Tos. "The 2020 WHO classification of soft tissue tumours: news and perspectives." *Pathologica* 113.2 (2021): 70.
- [12] J. Ker, Y. Bai, H. Y. Lee, J. Rao, & L. Wang (2019). "Automated brain histology classification using machine learning", *Journal of Clinical Neuroscience*, 66, pp. 239-245.
- [13] J. S. Lara, V. H. Contreras O, S. Otálora, H. Müller and F. A. González, 2020, September. "Multimodal latent semantic alignment for automated prostate tissue classification and retrieval.", In *Medical Image Computing and Computer Assisted Intervention - MICCAI 2020: 23rd International Conference, Lima, Peru, October 4-8, 2020, Proceedings, Part V* (pp. 572-581). Cham: Springer International Publishing.
- [14] Q. D. Vu, S. Graham, T. Kurc, M. N. N. To, M. Shaban, T. Qaiser, N. A. Koohbanani, Khurram, S. A., Kalpathy-Cramer, J., Zhao, T. and Gupta, R., 2019. Methods for segmentation and classification of digital microscopy tissue images. *Frontiers in bioengineering and biotechnology*, p.53.
- [15] S. Lin, A. J. Miao, J. Lu, S. Yu, Z. Y. Chiu, F. Richter and M. C. Yip, 2022. "Semantic-SuPer: A Semantic-aware Surgical Perception Framework for Endoscopic Tissue Classification, Reconstruction, and Tracking", *arXiv preprint arXiv:2210.16674*.
- [16] N. Dasari, and B. V. Reddy, 2023. "Multi-scale lung tissue classification for interstitial lung diseases using learned Gabor filters." *Microsystem Technologies*, pp. 1-9.
- [17] X. Liu, S. Ouellette, M. Jamgochian, Y. Liu, and B. Rao, 2023. "One-class machine learning classification of skin tissue based on manually scanned optical coherence tomography imaging." *Scientific Reports*, 13(1), p.867.
- [18] H. G. Nguyen, A. Blank, A. Lugli, and I. Zlobec, 2020, April. "An Effective Deep Learning Architecture Combination for Tissue Microarray Spots Classification of H&E Stained Colorectal Images." In *2020 IEEE 17th International Symposium on Biomedical Imaging (ISBI)* (pp. 1271-1274). IEEE.
- [19] Z. Xu, C. Dan, J. Khim, and P. Ravi Kumar, 2020, November. "Class-weighted classification: Trade-Offs and robust approaches", in *International Conference on Machine Learning*, pp. 10544-10554.
- [20] H. GM., M. K. Gourisaria, S. S. Rautaray, and M. Pandey, 2021. "Pneumonia detection using CNN through chest X-ray." *Journal of Engineering Science and Technology (JESTEC)*, 16(1), pp. 861-876.
- [21] R. Sharma, S. Das, M. K. Gourisaria, S. S. Rautaray and M. Pandey, 2020. A model for prediction of paddy crop disease using CNN. In *Progress in Computing, Analytics and Networking: Proceedings of ICCAN 2019* (pp. 533-543). Singapore: Springer Singapore.
- [22] A. Sahu, H. G. M., M. K. Gourisaria, "A Dual Approach for credit card fraud detection using neural network and data mining techniques", 2020, *IEEE 17th International Conference (INDICON)*, pp. 1-7.
- [23] S. Lin, A. J. Miao, J. Lu, S. Yu, Z. Y. Chiu, F. Richter and M. C. Yip, 2022. "Semantic-SuPer: A Semantic-aware Surgical Perception Framework for Endoscopic Tissue Classification, Reconstruction, and Tracking", *arXiv preprint arXiv:2210.16674*.
- [24] V. Singh, M. K. Gourisaria, H. GM, S. S. Rautaray, M. Pandey, M. Sahni, E. Leon-Castro and E. F. Espinoza-Audelo, 2022. "Diagnosis of intracranial tumors via the selective CNN data modeling technique." *Applied Sciences*, 12(6), p.2900.